Chalcogenide Letters Vol. 10, No. 1, January 2013, p. 1 - 10

DIELECTRIC AND IMPEDANCE STUDY OF OPTIMIZED CADMIUM SULPHIDE THIN FILM

K. S. OJHA[a*], R. L. SRIVASTAVA[b]
[a]*Institute of Engineering & Technology, Alwar-301030, India*
[b]*Institute of Technology and Management, GIDA, Gorakhpur, India*

Cadmium sulphide thin films are deposited by the spin coating technique onto well clean four alumina substrates. Out of four thin films, one film is untreated while the rest thin films are annealed at 100°C, 200°C and 300°C. The hexagonal phase formation of CdS thin films are confirmed by X-ray diffraction studies and the structural parameters like lattice parameter and crystallite size are calculated. The transmittance and absorbance spectra are recorded in the range of 500-1100 nm. The direct band gaps of the films are calculated. The frequency-dependent dielectric constant of cadmium sulphide (CdS) is investigated in the temperature range of 303-398 K and in the frequency range of 1 KHz-1 MHz by impedance spectroscopy.

(Received November 14, 2012; Accepted January 14, 2013)

Keyword: Cadmium sulphide, X-ray diffraction, Dielectric constant, Impedance spectroscopy, Band gap

1. Introduction

Cadmium sulphide is an n-type semiconductor and is being used in photo-resistance sensors, low cost solar cells for energy conversion, light emitting diodes, laser materials, optical waveguides and nonlinear optical devices [1-4]. It is a wide-direct-band gap semiconductor and has cubic or hexagonal structure. CdS used with the cadmium telluride semiconductor to fabricate solar cells given its optimal band gap energy (2.42 eV) for optical windows, while great importance in the optoelectronic applications and a diverse range of applications for thin films of this semiconductor including as waveguides, heterojunction devices and in thin-film electroluminescent displays in which it is the most commonly used host material [5]. Applications in optoelectronic methods or photovoltaic devices are another area receiving attention. In CdS based solar cells, the use of wider band gap materials such as ZnS or CdZnS could lead to decreases in window absorption losses and improvements in the short circuit current of the cells [5- 9].

During recent years, various properties such as structural, optical and dielectric properties of CdS thin films have been investigated by several researchers [10-14]. The crystalline quality of the CdS thin films plays an important role for electro-optical applications. Annealing of the thin films leads to improvement in the crystalline quality which is directly related to the dielectric loss and dielectric constant. Though various researchers have studied the dielectric properties of CdS thin films, a complete systematic study of various dielectric parameters in a wide range of frequency and temperature is still lacking. AC impedance spectroscopy allows the measurement of capacitance and loss tangent (tan δ) over a frequency range at various temperatures. Among various techniques such as vacuum evaporation, chemical bath deposition, spray pyrolysis and pulsed laser deposition, spin coating technique is inexpensive and simple. Spin coating technique

* Corresponding author: kspectra12@yahoo.co.in

is recognized as an important technique for the fabrication of multi-component thin films due to flexibility and the stoichiometric deposition of the materials. The aim of the present study is to optimize the structural and optical properties of CdS thin films and to study the dielectric and impedance properties of optimized CdS thin film.

2. Experiemntal

CdS thin films are deposited on alumina substrates by spin coating technique using cadmium acetate [$(CH_3COO)_2$ Cd.2H2O] as Cd^{++} ion source and thiourea [$CS(NH_2)_2$] as S^{-2} ion source with cadmium to sulphur (Cd:S) molar ratio 3:5. 0.6 M cadmium acetate and 1 M thiourea solutions are taken in a beaker, stirred for 8 hours at 100°C. As the reaction is started, the reaction system gradually changed from transparent to light yellow and after completion of the reaction this turns bright yellow. The pH of the final solutions is found to be 5.6. The solution is left overnight for stabilization. The CdS thin films are deposited on alumina substrates. An alkaline solution of ammonia is used to adjust the pH of the solution. The CdS thin films are deposited on four substrates for 30 seconds at 3000 rpm. After deposition, the substrates are removed and thoroughly washed in doubly distilled water. Out of four samples, three samples are annealed at 100°C, 200^0C and 300^0C for 2 hours.

3. Results

3.1 Structural Study

The XRD patterns of un-annealed and annealed CdS thin films at 100ºC, 200 ºC and 300 ºC are recorded using Rigaku Miniflex X- ray diffractometer with CuK_{α} **(**λ=1.540598**)** over the range 10° to 80° and are shown in Fig. 1. Only one peak at 2θ=26.43° corresponds to (002) peak of hexagonal CdS is observed for un-annealed CdS thin film. The XRD pattern of the CdS thin film annealed at 100°C shows two sharp peaks at 2θ=26.43° and 28.04° corresponding to (002) and (101) planes while the XRD pattern of the CdS thin film annealed at 200°C shows four peaks at 2θ=26.43°, 28.04°, 47.79° and 51.91° corresponding to (002), (101), (103) and (112) planes of hexagonal CdS thin films. However, after annealing at 300°C, six strong diffraction peaks at 2θ values of approximately 24.83°, 26.48°, 28.11°, 43.72°, 47.79° and 51.91° are observed which correspond to the diffraction lines produced by the (100), (002), (101), (110), (103) and (112) crystalline planes of CdS thin film. From the pattern, it is clear that all the films grown on alumina substrate are of polycrystalline and single phase. The lattice parameters, calculated from the prominent peaks are found to be 4.17Å and 6.73Å. The crystallite sizes are calculated by using the formula

$$D = 0.9\lambda \Big/ (\beta Cos\ \theta)$$

where λ is the wavelength of the used X- ray, β is the full width at half maximum (FWHM) of the corresponding peak and θ is the Bragg angle. The average crystallite size is found to be 41.00 nm, 41.28 nm, 41.37 nm and 41.49 nm respectively for the un-annealed and CdS thin films annealed at 100°C, 200°C and 300°C. The increase in grain size with increasing annealing temperature attributed to the improvement in the degree of the crystallinity of the films.

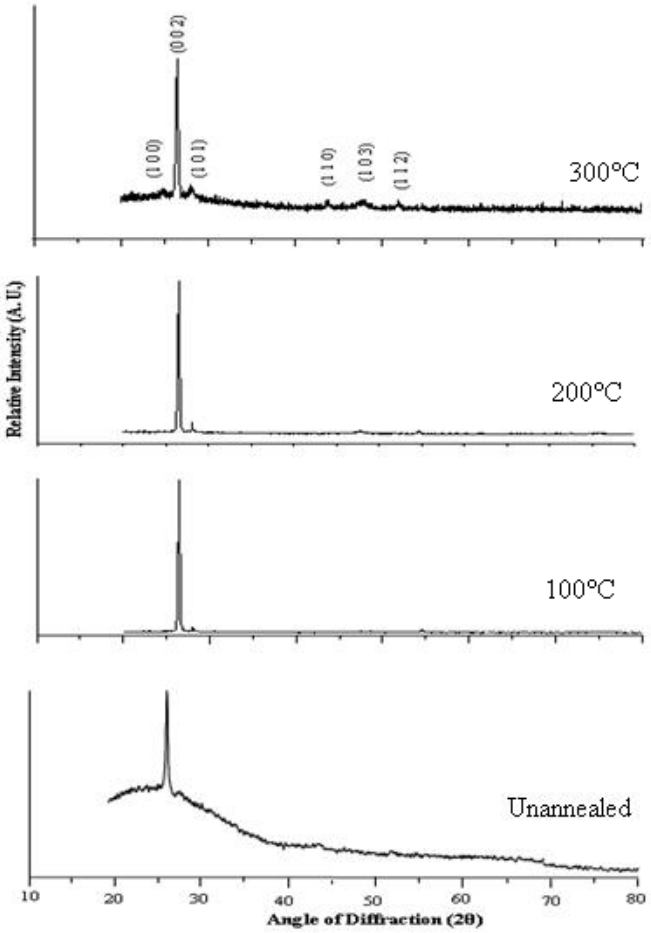

Fig. 1. XRD pattern of un-annealed and annealed CdS thin films

3.2. Optical Study

The transmittance and absorbance spectra for the un-annealed and CdS thin films annealed at 100°C, 200°C and 300°C are recorded in the wavelength scanning mode using Shimadzu UV-Vis spectrophotometer (Model: 1700). The optical properties of the CdS thin film are very important in optimizing the growth conditions to be used as a window layer of solar cells. The wavelength dependence transmittance and absorbance curves of CdS thin films annealed at 100°C, 200°C and 300°C are shown in Figure (2a) and (2b). The average transmittance of the films decreases after annealing which may be attributed to the absorption of light and development of micro-crystallites. The absorption coefficient α is related to the incident photon energy hν as:

$$\alpha = \frac{K\left(h\nu - E_g\right)^{n/2}}{h\nu}$$

where K is a constant, E_g is the optical bandgap, and n is equal to **1**for direct bandgap material such as CdS. The bandgap is determined for each film by plotting $(\alpha h\nu)^2$ versus $h\nu$ and then extrapolating the straight line portion to the energy axis. The plot of $(\alpha h\nu)^2$ versus $h\nu$ in the absorption region indicates direct allowed transition in the film material which is shown in the figure 3(a-d). The evaluated band gap energies are 2.55 eV, 2.49 eV, 2.44eV and 2.27eV respectively for the un-annealed and CdS thin films annealed at 100°C, 200°C and 300^0C

respectively which shows that bandgap decreases with increasing annealing temperature for CdS thin films due to decrease in dislocation density and improved crystallinity.

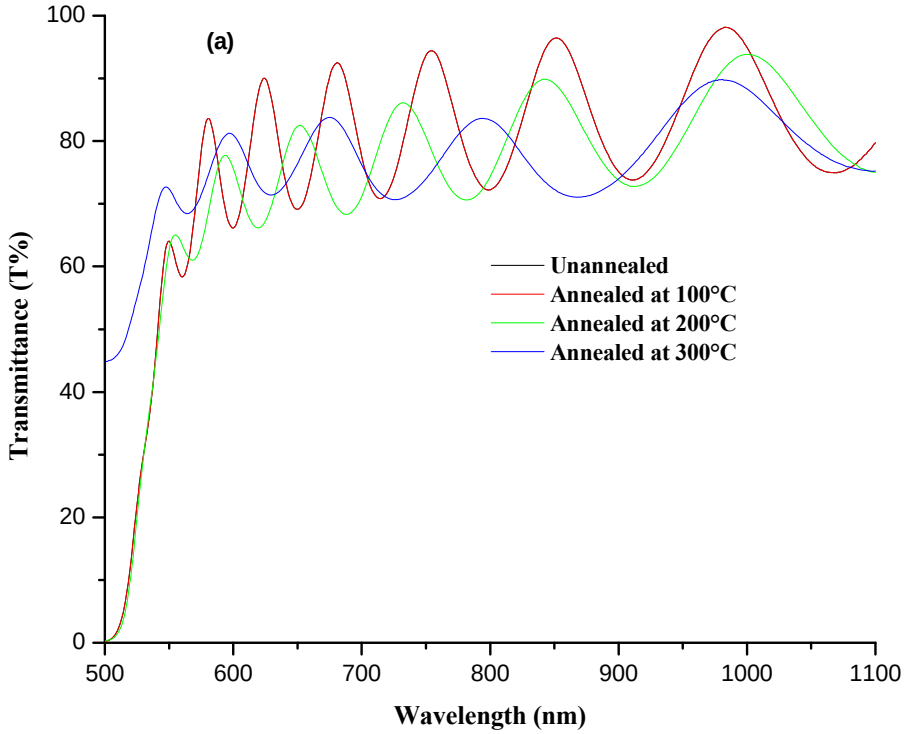

Fig. 2(a). Transmittance spectra of un-annealed and annealed CdS thin films

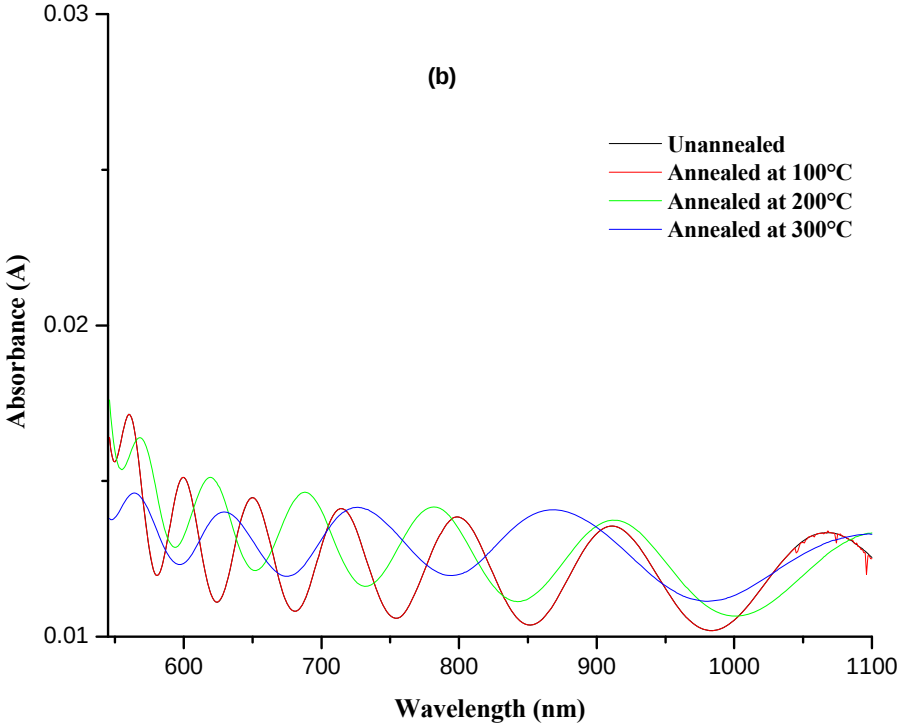

Fig. 2(b). Absorbance spectra of un-annealed and annealed CdS thin films

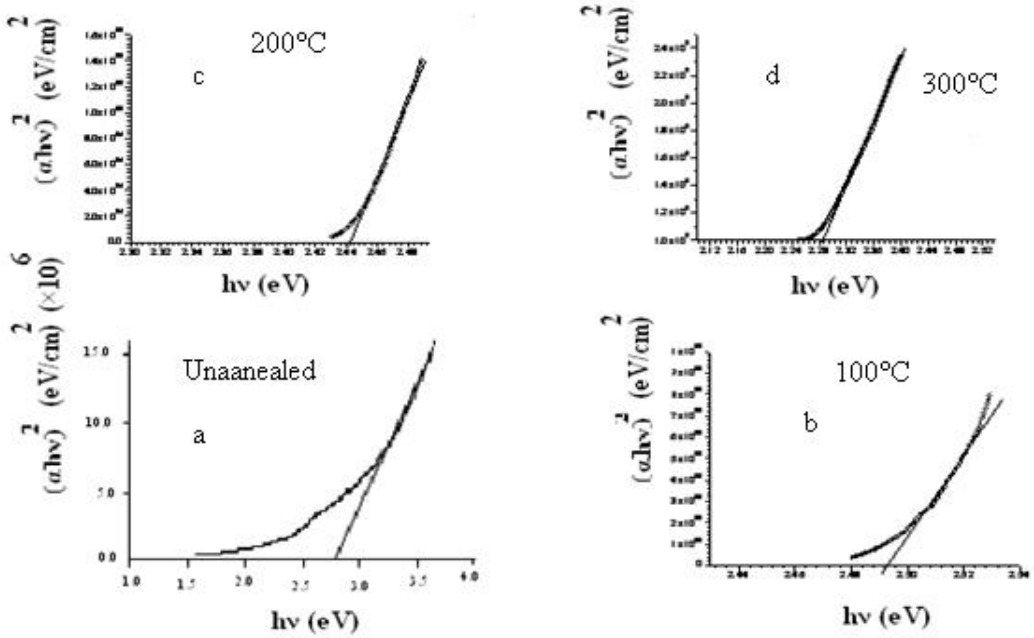

Fig. 3. Plot of $(\alpha hv)^2$ vs hv for un-annealed and annealed CdS thin films

3.3 Dielectric and Impedance Studies:

Figure 4 (a) shows the temperature dependence of dielectric constant at different frequencies of optimized CdS thin film annealed at 300°C. The dielectric constant at low frequencies starts from high value and decreases with increase in temperature. As the temperature further increases, the dielectric constant values start increasing. The high value of dielectric constant at low temperature attributed to space charge polarization whereas at higher temperature and low frequencies it may be associated with defect related conduction processes. Figure 4(b) represents the temperature dependence of dielectric loss which has similar behaviour as that of dielectric constant; however frequency dependent loss peak is clearly descramble at around 110^0C. The increase in the peak value of tan δ with the increase in temperature indicates that the number of charge carriers increases by thermal activation and the position of loss peak shifts to higher frequency with increasing temperature. Such behaviour of the loss tangent in CdS thin film is supposed to be due to the existence of the broad spectrum of the relaxation times.

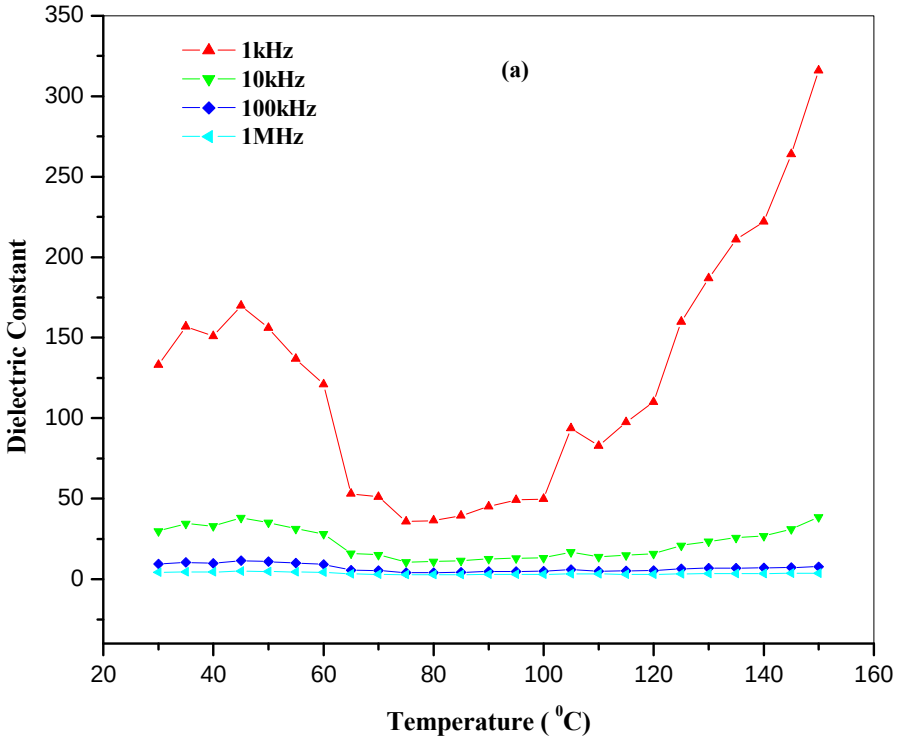

Fig. 4. (a) Temperature dependent dielectric constant of CdS thin film annealed at 300°C

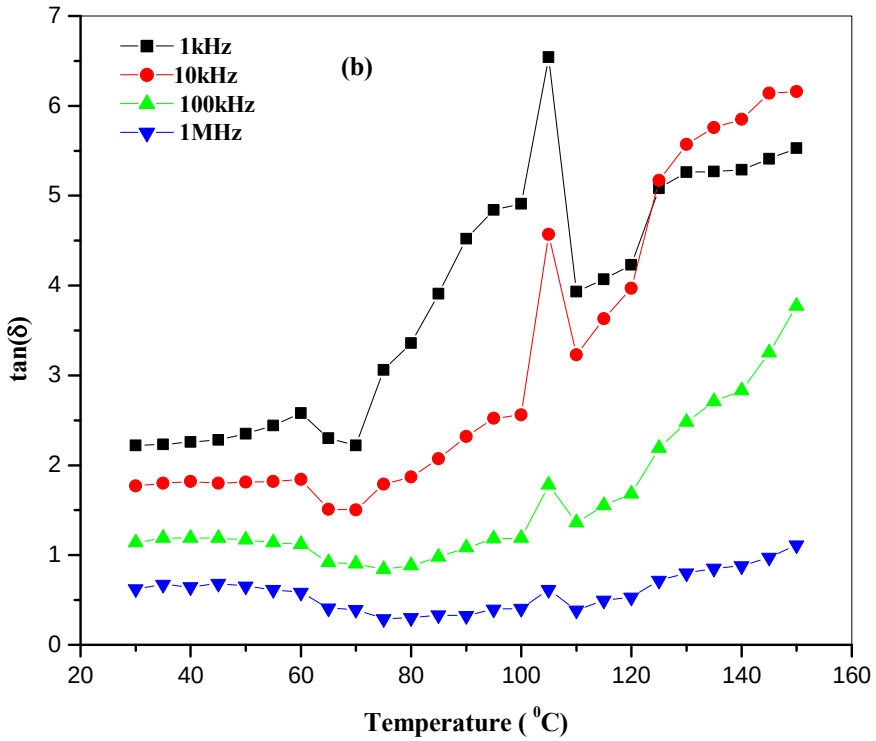

Fig. 4. (b) Temperature dependent dielectric loss of CdS thin film annealed at 300°C

Figure 5 (a) and (b) show frequency dependence real (ε') and imaginary (ε") part of dielectric constant respectively. Both ε' and ε" show dispersion at low frequencies and gets almost saturated at higher frequencies. A relaxation is observed in the entire temperature range as a gradual decrease in ε' with increasing frequency. At very low frequencies, dipoles follow the field.

As the frequency increases, dipoles begin to lag behind the field and ε' slightly decreases. At very high frequencies, dipoles can no longer follow the field.

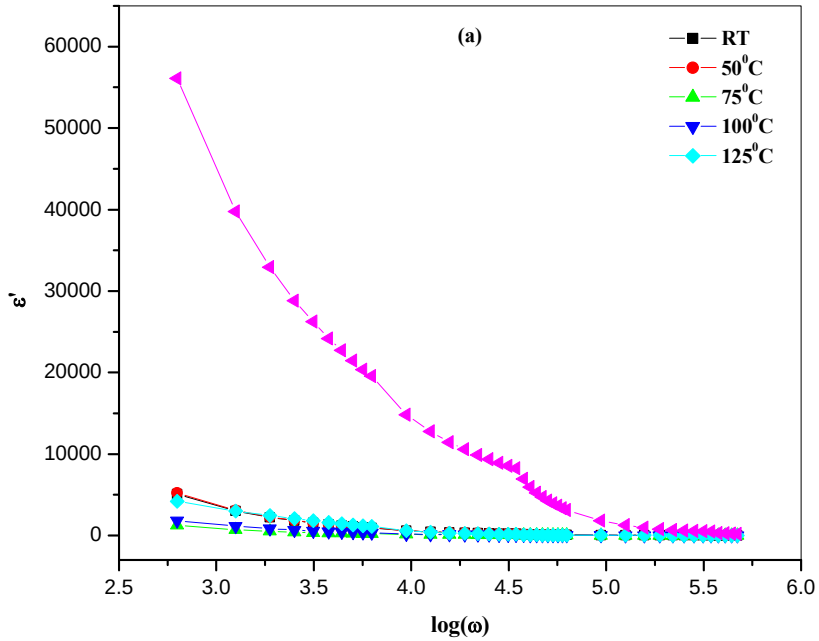

Fig. 5. (a) Frequency dependence of dielectric constant of CdS thin film annealed at 300°C

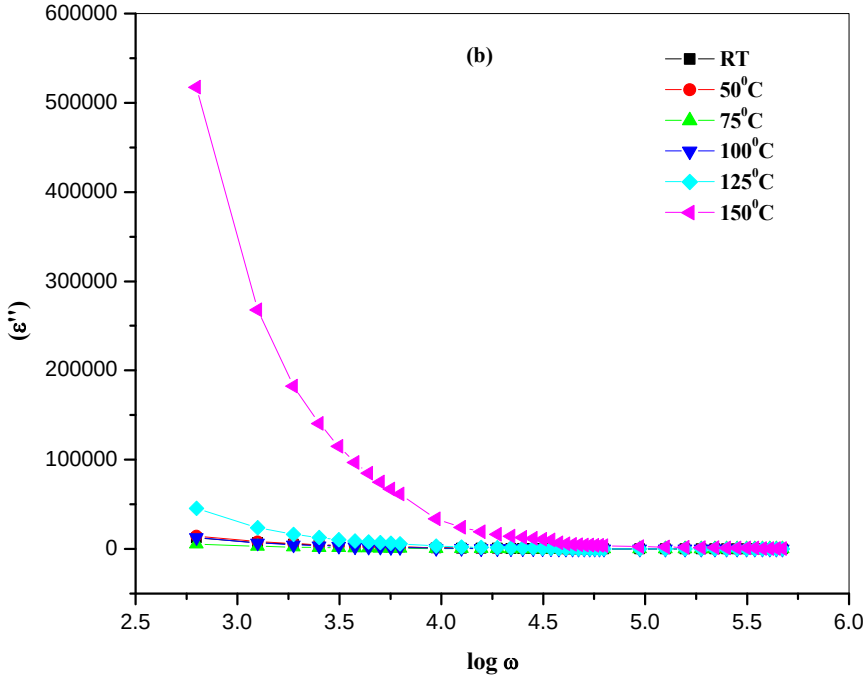

Fig. 5. (b) Frequency dependence of dielectric loss of CdS thin film annealed at 300°C

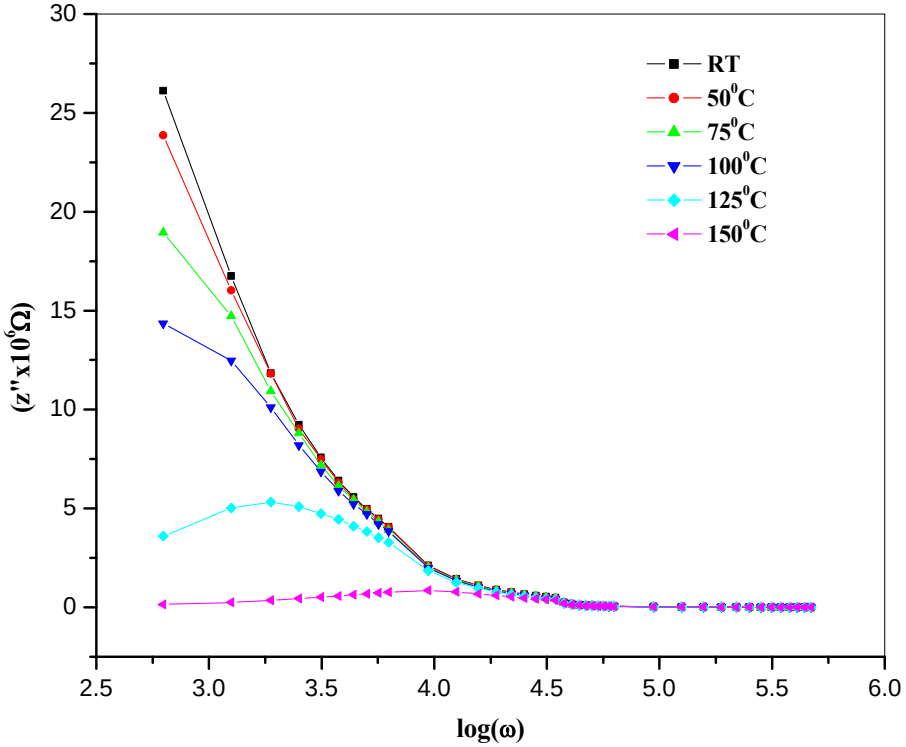

Fig. 6. Variation of imaginary part of impedance as a function of frequency at different temperatures of CdS thin film annealed at 300°C

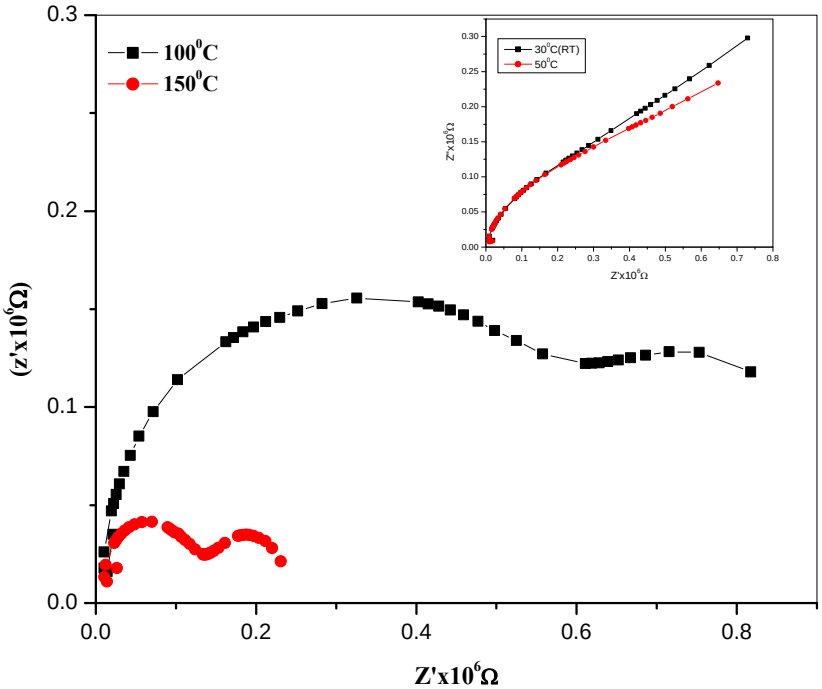

Fig. 7. Nyquist plots for CdS thin film at 100°C and 150°C (Inset shows the same for low temperatures 30⁰C and 50⁰C) annealed at 300°C

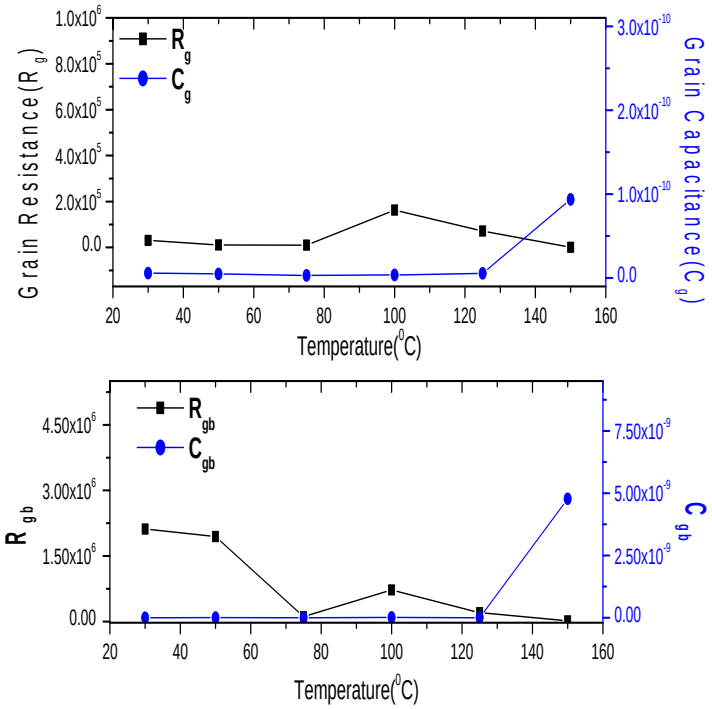

Fig. 8. Temperature dependence of R_g, C_g and R_{gb}, C_{gb} for CdS thin film annealed at 300ºC

The nature of material response and process involved is explored using the impedance behaviour. The frequency dependence of imaginary part of impedance (Z") is shown in figure 6. At temperature above 100^0C, the impedance loss peak starts appearing and shifts towards the higher frequency with increasing temperature showing that the resistance is decreasing. Also the magnitude of Z" decreases with increasing frequency indicating that the behaviour is of semiconductor type. The imaginary part of impedance (Z") is plotted against the real part of impedance (Z') at temperature 100ºC and 150^0C and is shown in figure 7. For a single-phase polycrystalline material, two semicircular arcs are obtained in the complex plane plot, which can be explained as two parallel RC elements connected in series, one branch is associated with the grain and other with the grain boundary of the CdS thin film as shown in figure 8.

4. Conclusions

The structural and optical properties of cadmium sulphide films, prepared by pulsed laser deposition technique, are optimized and the polycrystalline single phase CdS thin film with good crystallinity is observed at 300ºC. The evaluated crystallite sizes increase from 41.00 nm to 41.49 nm and the band gap decreases from 2.55eV to 2.27eV with the increase of annealing temperature from room temperature to 300ºC. The values of ε' and ε" show dispersion at low frequencies and become almost saturated at higher frequencies. The dispersion increases with increase in temperature due to space charge accumulation effect. The impedance of material is due to contribution of both grain and grain boundaries. The analysis of the real and imaginary part of impedance with frequency shows a distribution of relaxation times as confirmed by Nyquist plot.

References

[1] Y. Kashiwaba, J. Sato, T. Abe, Appl. Surface Sci. **162**, 212 (2003)
[2] E. Bacaksiz, V. Novruzov, H. Karel, E. Yanmaz, M. Altunbas, A. I. Kopya, J. Phys. D: Appl. Phys., **34,** 3109 (2001)

[3] B. Ullrich, D. M. Bagnall, H. Sakai, Y. Segawa, J. of Luminescence, **87-89**, 1162 (2000)
[4] K. Senthil, D. Mangalarj, S. K. Narayandass, Appl. Surface Sci. **169-170**, 476 (2001)
[5] R.B. Kale, C.D. Lokhande, Appl. Surf. Sci, **252**, 929 (2005)
[6] H.Tang, Mi Yan, Hui Zhang, M.Xia, DerenYang, Materials letter **59**, 1024 (2005)
[7] P. Tyagi and A. G. Wedeshwar, Bull. Mater. Sci. **24 (3)**, 297 (2001)
[8] S. Shrivastava and B. Verma; Cryst. Res. Technol. **42(5)**, 466 (2007)
[9] J. Barman, J. P. Borah, K. C. Sarma; Chalcogenide Letters **5 (11)**, 265 (2008)
[10] R. Bhattacharya and S. Saha, Pramana J. Phys. **71**, 187 (2008)
[11] M. Maleki, M. S. Ghamsari, S. Mirdamadi and R. Ghasemzadeh, Semiconductor Physics: Quantum Electronics & Optoelectronics **10**, 30 (2007)
[12] S. Tiwari and S. Tiwari, Cryst. Res. Technol. **41**, 78 (2006)
[13] H. Zhang, D. Yang, X. Ma, Y. Ji, S. Z. Li and D. Que, Mater. Chem. Phys. **93**, 65 (2005)
[14] S. M. Zou, Phys. Status Solidi A **200**, 423 (2003)